THE JOURNAL OF PHYSICAL CHEMISTRY Letters

Letter

pubs.acs.org/JPCL

Optically Controlled Electron-Transfer Reaction Kinetics and Solvation Dynamics: Effect of Franck–Condon States

Kriti Gupta,[†,⊥] Aniket Patra,[‡] Kajal Dhole,[§] Alok Kumar Samanta,[*,∥,⊥] and Swapan K. Ghosh[∥,⊥]

[†]Faculty of Science and Technology and MESA+ Institute for Nanotechnology, University of Twente, 7500 AE Enschede, The Netherlands

[‡]Department of Physics and Astronomy, Rutgers, The State University of New Jersey, New Jersey 08854-8019, United States

[§]Research Reactor Services Division, Bhabha Atomic Research Centre, Mumbai 400085, India

[∥]Theoretical Chemistry Section, Bhabha Atomic Research Centre, Homi Bhabha National Institute, Mumbai 400085, India

[⊥]UM-DAE Center of Excellence in Basic Sciences, Kalina Campus, Mumbai 400098, India

ABSTRACT: Experimental results for optically controlled electron-transfer reaction kinetics (ETRK) and nonequilibrium solvation dynamics (NESD) of Coumarin 480 in DMPC vesicle show their dependence on excitation wavelength λ_{ex}. However, the celebrated Marcus theory and linear-response-theory-based approaches for ETRK and NESD, respectively, predict both of the processes to be independent of λ_{ex}. The above said lacuna in these theories prompted us to develop a novel theory in 1D space, where the effect of innumerable Franck–Condon states is included through λ_{ex}. The present theory not only sheds light on the origin of failure of the existing theories but also gives the correct trend for the effect of λ_{ex} on ETRK and NESD. More importantly, the calculated results of NESD are in excellent agreement with the experimental results for different values of λ_{ex}. The new theory will therefore advance the knowledge of scientific community on the dynamics of photoinduced nonequilibrium processes.

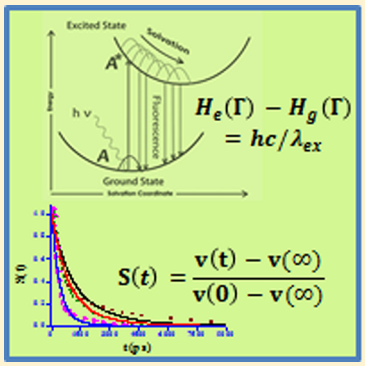

The control of molecular dynamics and rate of chemical reactions by tuning thermodynamic and kinetic parameters has provided recurring themes of research in physics and chemistry, in which theoretical predictions[1−16] have been consistent with experimental observations. With the advent of laser spectroscopy, more precise control of dynamical processes in condensed phase, for example, electron transfer reaction kinetics (ETRK) (Figure 1) and nonequilibrium solvation dynamics (NESD) (Figure 2), by proper tuning of the optical excitation wavelength λ_{ex} has created immense interest in chemical physics community in recent times. Experiments conducted for optically controlled ETRK[17−21] and NESD[22−24] show their dependence on the excitation wavelength λ_{ex}. However, the celebrated Marcus theory[16] and other theories[11−15] developed based on the same for ETRK, linear response theory[1−10] for NESD, show that both ETRK and NESD should be independent of λ_{ex}. In the case of Marcus theory[16] for electron transfer, it is assumed that the system initially and at the critical point where electron transfer does take place always remains in thermal equilibrium. However, in the case of optically created innumerable Franck–Condon state (nonequilibrium state (Figure 1b)) and the critical configuration (X* of Figure 1), electron transfer does take place in the nonequilibrium state instead of the equilibrium one. In this case, the overall ETRK depends on the time taken for the journey from the initially prepared Franck–Condon state (Figure 1b) to the critical configuration (X* of Figure 1). Again, initially prepared Franck–Condon states (nonequilibrium state (Figure 1b)) are different for different λ_{ex}. We can therefore expect the ETRK should depend on λ_{ex}. According to the linear response theory, NESD is identical to the dynamics of equilibrium ensemble average of energy gap fluctuation relaxation. Therefore, according to this theory, optically controlled NESD (Figure 2) should not depend on λ_{ex} because optically controlled NESD depends on the time taken by the system for the journey from the initially prepared innumerable Franck–Condon states (nonequilibrium state (A* of Figure 2)) to the bottom of excited-state potential energy surface. Again, initially prepared innumerable Franck–Condon states (nonequilibrium state (A* of Figure 2)) are different for different λ_{ex}. We therefore expect the optically controlled NESD to depend on λ_{ex}. The major difficulties in the Marcus, linear response, and other theories[1−16] developed based on these theories are that there is no provision to include an optical tuning parameter such as the photoexcitation wavelength λ_{ex} as an input parameter; therefore, these theories fail to explain the λ_{ex} dependence of ETRK[17−21] and NESD[22−24] observed in experiment. The failure of the approximate existing theories[1−16] prompted us to develop a novel unified theory that takes into account the effect of not only the thermodynamic parameters but also the effect of innumerable Franck–Condon states through the single parameter λ_{ex}. This unified theory is

Received: July 26, 2017
Accepted: September 5, 2017
Published: September 5, 2017

ACS Publications © 2017 American Chemical Society

DOI: 10.1021/acs.jpclett.7b01938
J. Phys. Chem. Lett. 2017, 8, 4545−4549

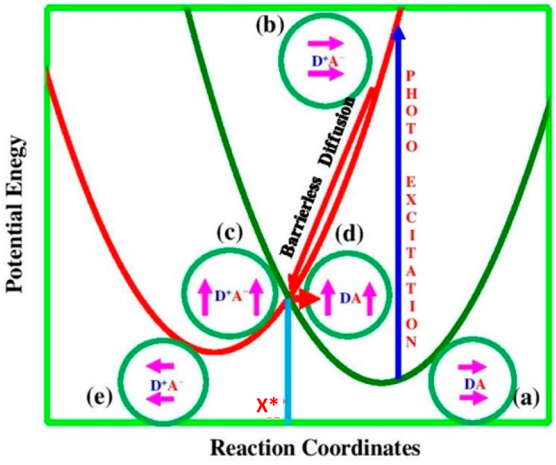

Figure 1. (a) Equilibrium state (before photoexcitation) for DA (donor−acceptor pair) and solvent at a particular configuration (indicated by arrow). (b) Non-equilibrium initial state (after photoexcitation) for D^+A^- and solvent at the same configuration as in panel a. (c) Non-equilibrium state (before ET) at transition point for D^+A^- and solvent at new different configuration (indicated by different arrow). (d) Non-equilibrium state at transition point (after ET) for DA and solvent at the same configuration as in panel c. (e) Equilibrium state for D^+A^- and solvent at new different configuration (indicated by different arrow).

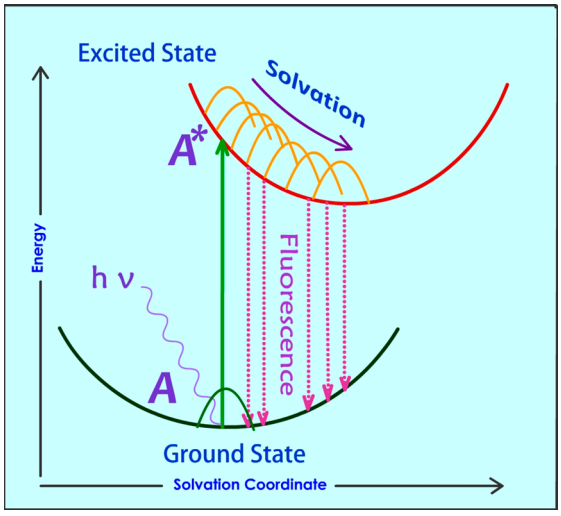

Figure 2. Schematic illustration of the potential energy surfaces involved in solvation dynamics in DMPC vesicle (Figure 4). Lower surface represents the solute (A) (Coumarin 480) and solvent in the different region of DMPC vesicle, while the upper surface represents the solute (A*) in excited state and the solvent in the same region as in the ground state. As the solvation proceeds, the solute (A*) particles emit light in the form of fluorescence, with continuously decreasing frequency $\nu(t)$ (shown by vertical downward arrow).

then applied to the two most important nonequilibrium processes, viz. photoinduced NESD[22−24] of Coumarin 480 in microenvironments of dimyristoyl-phosphatidylcholine (DMPC) lipid vesicle and ETRK[17−21] in condensed phase to explain the effect of λ_{ex} on these nonequilibrium processes observed in experiment.

To study the effect of λ_{ex} on NESD and ETRK, we first derive the kinetic equation in 1D space for the probability distribution $g(a,t)$, where $g(a,t)$ represents the probability of finding the reaction coordinate or solvation coordinate to have the value a at time t. The kinetic equation for $g(a,t)$ is derived by employing the projection operator methodology developed by Zwanzig[25] and Garcia-Colin et al.[26] and generalized further by us.[27−30] The derivation leads to the final simplified kinetic equation

$$\frac{\partial g(a,t)}{\partial t} = D\frac{\partial}{\partial a}\left[\frac{\partial}{\partial a} + \beta\frac{\partial V_{\text{eff}}(a)}{\partial a}\right]g(a,t) - k_0\delta(a-a^*)g(a,t) \quad (1)$$

where k_0 represents the intrinsic rate constant for ETRK at the transition point where electron transfer takes place. To study the solvation dynamics, the above kinetic equation will be used with $k_0 = 0$. Here D and $V_{\text{eff}}(a)$ represent,[25−30] respectively, the diffusion constant and effective potential in solvation coordinate ($k_0 = 0$ of eq 1) or reaction coordinate space for ETRK ($k_0 \neq 0$ of eq 1). Here β denotes the inverse temperature. In the a space, it can be shown that the initial nonequilibrium distribution function becomes simply a 1D Dirac delta function

$$g(a,0) = \delta\left(a - \frac{hc}{\lambda_{ex}}\right) \quad (2)$$

where h and c represent the Planck constant and the velocity of light. Here the effect of innumerable Franck−Condon states (Figure 1b and A* of Figure 2) enters through λ_{ex} (eq 2). Again, the effect of λ_{ex} on $g(a,t)$ is included through $g(a,0)$ (eq 2). However, in the case of Marcus theory[16] for electron-transfer reaction and linear-response-theory-based[1−10] approach for NESD, it is assumed that the system remains initially in thermal equilibrium state instead of nonequilibrium (eq 2) one. Because of the initial thermal equilibrium distribution function adopted in Marcus, linear response, and other existing theories,[1−16] they fail to explain the effect of λ_{ex} on ETRK and NESD observed in experiment. The unified theory (eqs 1 and 2) developed here is now to be employed to explain the effect[17−24] of λ_{ex} on the two very important classes of non equilibrium processes, viz. optically controlled ETRK[17−21] and NESD[22−24] of Coumarin 480 in DMPC lipid vesicle.

In the case of ETRK, we consider a many-particle system consisting of solute DA (donor−acceptor system) (Figure 1a) and solvent, which are in thermal equilibrium. The ion-pair D^+A^- in the solvent medium (Figure 1b) is formed by shining light of ultrashot laser pulse. According to Franck−Condon principle, the nuclear configuration in the ground state (Figure 1a) and ion pair state (Figure 1b) remains the same. When light is switched off, the system starts the journey toward the equilibrium state (Figure 1a) in the downhill potential of the ion pair D^+A^-. During its journey, when the system reaches the critical configuration $H_e(\Gamma) = H_g(\Gamma)$) (X* of Figure 1, corresponding to $a^* = 0$ in eq 1), the electron transfer takes place with an intrinsic rate constant k_0. Here $H_g(\Gamma)$ and $H_e(\Gamma)$, respectively, represent the Hamiltonian (H^{DA}) of the solute−solvent system in the ground (DA and solvent) and Hamiltonian ($H^{D^+A^-}$) of ion-pair state (D^+A^- in the solvent medium).

To explain the experimental observation[17−21] that with an increase in λ_{ex} the rate of ETRK increases, we consider here a simple theoretical model consisting of a multidimensional space spanned by the solvent polarization $P(\mathbf{r})$ and the low-frequency

DOI: 10.1021/acs.jpclett.7b01938
J. Phys. Chem. Lett. 2017, 8, 4545−4549

vibrational coordinate q as well as the high-frequency quantum mode (ω). Thus one has

$$H^{D^+A^-} = \int f(\mathbf{r})\mathbf{P}(\mathbf{r})\cdot\mathbf{P}(\mathbf{r})\,d\mathbf{r} - \int \mathbf{P}(\mathbf{r})\cdot\mathbf{E}(\mathbf{r})\,d\mathbf{r} + \frac{1}{2}(q+q_0)^2 + \left(n^e + \frac{1}{2}\right)\hbar\omega + \Delta E^{el} \quad (3)$$

$$H^{DA} = \int f(\mathbf{r})\mathbf{P}(\mathbf{r})\cdot\mathbf{P}(\mathbf{r})\,d\mathbf{r} + \frac{q^2}{2} + \left(n^g + \frac{1}{2}\right)\hbar\omega \quad (4)$$

where $\mathbf{E}(\mathbf{r})$ represents the electric field at the point $\mathbf{r}$ due to the ion pair D^+A^- and the function $f(\mathbf{r})$ takes into account the effect of finite size of the solvent molecules. Here ΔE^{el} represents the electronic energy change due to the transition $DA \rightarrow D^+A^-$ and can be expressed $\Delta E^{el} = \lambda_T - \Delta G$, where $\lambda_T$and ΔG represent, respectively, the solvent reorganization energy and free energy of the charge recombination reaction $D^+A^- \rightarrow DA$.

The vibrational quantum numbers n^g and n^e, respectively, represent the ground (DA and solvent) and excited state (D^+A^- in the solvent medium). The experimentally measurable quantity $p(t,\varepsilon_0)$ represents the concentration of the unreacted species D^+A^- at time t and can be expressed for the model potential defined in eqs 3 and 4 and using the eq 1 as

$$p(t,\varepsilon_0) = \int_{-\infty}^{\infty} da\, g(a,t) = \sum_{n=0}^{\infty} C_n(t) q_n(\varepsilon_0) \quad (5)$$

where the equation for $C_n(t)$ is defined as

$$\frac{dC_j(\tau)}{d\tau} = -jC_j(\tau) - \tau_L\sqrt{\frac{\beta}{4\lambda_T}}\,k_0 \exp[-(\varepsilon^*)^2] \times \sum_{n=0}^{\infty} C_n(\tau) q_n(\varepsilon^*) q_j(\varepsilon^*) \quad (6)$$

with $\varepsilon_0 = (\Delta G + \lambda_T - \hbar\omega + hc/\lambda_{ex})\sqrt{\frac{\beta}{4\lambda_T}}$, $\varepsilon^* = (\Delta G + \lambda_T)\sqrt{\frac{\beta}{4\lambda_T}}$, and $\tau = t/\tau_L$, where τ_L represents the solvent orientation relaxation time. Here $q_n(\varepsilon_0)$ represents the normalized Hermite polynomials. To explain the effect of excitation wavelength on ETRK observed in experiment,[17−21] we consider here a barrierless processes ($\Delta G + \lambda_T = 0$) for electron-transfer reaction and solve the first-order coupled differential eqs 5 and 6 numerically for three different excitation wavelengths, λ_{ex} = 480, 620, and 800 nm, considered in experimental studies,[17−21] and the parameters used are ΔG = −4.0 eV and J = 0.3 eV. Here J^2, which is defined through k_0 as $k_0 = \left(\frac{4\pi^2}{h}\right)J^2$, represents the electron-transition probability at the transition point (X* in Figure 1). The calculated results are plotted in Figure 3, from which it is clear that the decay of the excited-state population $p(t,\varepsilon_0)$ becomes faster with increase in λ_{ex}, which is consistent with the experimental observations.[17−21] However, the Marcus theory[16] and all other theories[11−15] developed based on this principle predict that the ETRK rate should be independent of λ_{ex} and thus fail to explain the experimental observation[17−21] (Figure 3).

Here the ETRK rate k_0 (at X* of Figure 1) is very large in comparison with the diffusive dynamics (Figure 1b→c) of the solute (D^+A^-)−solvent system, and the overall ETRK rate is thus dictated by diffusion dynamics (Figure 1b→c) only. In this

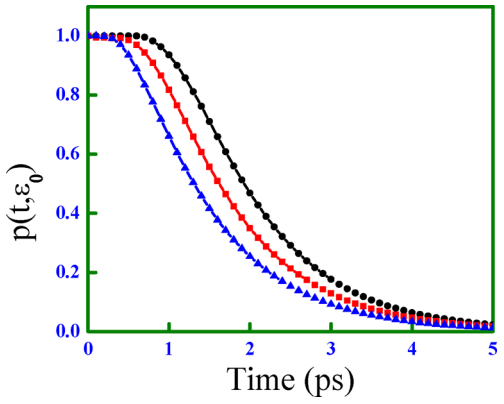

Figure 3. Plot of the excited-state population decay function $p(t, \varepsilon_0)$ versus time t (in ps) based on the new relation (eqs 5 and 6) for the parameters: ΔG = −4.0 eV, T = 300 K, τ_L = 0.3 ps, and J = 0.47 eV and selected values of excited wavelength λ_{ex} = 480 nm (○), λ_{ex} = 620 nm (□), and λ_{ex} = 800 nm (△), considered in the experimental[17−21] studies of ETRK.

case, with decrease in λ_{ex}, the system is placed far away (Figure 1b) from the reaction position, that is, the sink position (X* in Figure 1); therefore, the system takes a longer time to reach the same position (X* in Figure 1). Hence, the population of the solute (D^+A^-) represented by $p(t,\varepsilon_0)$ decays slowly, with consequent decrease in the ETRK rate.

We now consider NESD, focusing first on a solute A in a ground electronic state dissolved in a solvent, and the solute is then excited to a different electronic state A* (Figure 2) through optical excitation. As the molecule A* and solvent molecules relax on the excited-state potential surface, A* can undergo a transition to the ground state (A in Figure 2) by photoemission. The change in the energy of the solute is measured experimentally in terms of the time-dependent fluorofrequency $\nu(t)$ (represented by vertical dotted lines in Figure 2) leading to the fluorescence spectrum. The experimentally observed quantity nonequilibrium solvation time-correlation function (NSTCF) $S(t)$ is defined in terms of the emitted light frequency $\nu(t)$ and $g(a,t)$ as

$$S(t) = \frac{\nu(t) - \nu(\infty)}{\nu(0) - \nu(\infty)} = \frac{\int_{-\infty}^{\infty} da\, a\, g(a,t) - \int_{-\infty}^{\infty} da\, a\, g(a,\infty)}{hc/\lambda_{ex} - \int_{-\infty}^{\infty} da\, a\, g(a,\infty)} \quad (7)$$

and is used to elucidate the underlying molecular motions involved in the relaxation of the solvent in response to the solute excitation. Here $g(a,t)$ (k_0 = 0 of eq 1) represents the distribution function for solvation dynamics.

To explain the experimental results[22−24] and the origin for the hidden break down of linear response theory[10] and other existing theories[1−9] developed based on this, we consider an anharmonic potential in solvation coordinate space (a), viz.

$$V_{eff}(a) = \frac{1}{4\lambda_T}(a - k_m)^2 + \theta(a - k_m)^4 \quad (8)$$

where θ is the anharmonicity parameter. Now combining eqs 1, 7, and 8 for k_0 = 0 and assuming θ to be small, after some algebra, we obtain the new expression for $S(t)$ given by

DOI: 10.1021/acs.jpclett.7b01938
J. Phys. Chem. Lett. 2017, 8, 4545−4549

$$S(t) = \frac{1}{2}(L\exp[A\tau] - M\exp[-B\tau]) - \beta\frac{\left(\left(\frac{hc}{\lambda_{ex}}\right) - k_m\right)^2}{6\lambda_T}\frac{\kappa}{\kappa_1}(\exp[A\tau] - \exp[-B\tau]) \quad (9)$$

where $\kappa = \frac{24(\lambda_T)^2\theta}{\beta}$, $\kappa_1 = 2\sqrt{\frac{1}{4} - \kappa}$, $A = \kappa_1 - 2$, $L = \left(\frac{1}{\kappa_1} + 1\right)$, $M = \left(\frac{1}{\kappa_1} - 1\right)$, and $B = \kappa_1 + 2$. It is clear from eq 9 that $S(t)$ is independent of λ_{ex} for harmonic potential ($\theta = 0$), which is in accord with linear response theory[10] and other existing theories'[1−9] prediction. However, in the case of anharmonic potential ($\theta \neq 0$), eq 9 and experimental results[22−24] suggest that $S(t)$ depends on the excitation wavelength, λ_{ex}, indicating the breakdown of linear response theory[10] and other existing theories.[1−9] Equation 9 is now to be employed to explain the effect of excitation wavelength λ_{ex} on solvation dynamics of coumarin 480 in a heterogeneous medium[22−24] of DMPC lipid vesicle (Figure 4). To reproduce the results predicted by

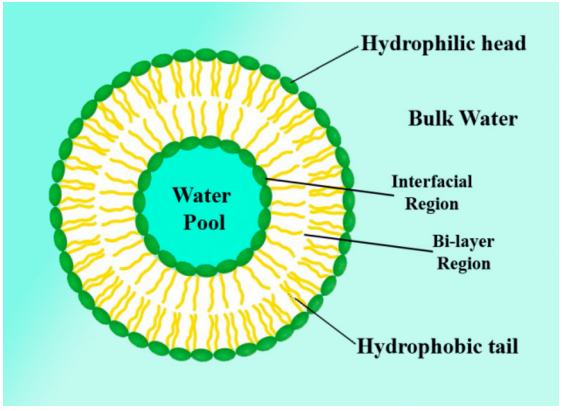

Figure 4. Schematic representation of heterogeneous microenvironments of dimyristoyl-phosphatidylcholine (DMPC) lipid vesicle. There are four possible locations of the probe molecule Coumarin 480: bulk water, water pool, inner interfacial region, and hydrocarbon-like region (bilayer region).

experiment[22] we consider the parameters k_m = 4.0 eV, reorganization energy λ_T = 0.4 eV, T = 300 K, anharmonicity parameter κ = 0.05, and the solvent relaxation time τ_L = 2200 ps corresponding to the excitation wavelength λ_{ex} = 390 and 410 nm and τ_L = 1100 ps for λ_{ex}= 420 nm. The results obtained for $S(t)$ based on eq 9 are plotted in Figure 5 for λ_{ex} = 390, 410, and 420 nm.

It is obvious from Figure 5 that $S(t)$ depends on the excitation wavelength, indicating the breakdown of linear response theory hypothesis[10] and other existing theories.[1−9] The calculated results are in excellent agreement with the experimental ones. It is clear from Figure 5 that although $S(t)$ is different for two different excitation wavelengths viz. λ_{ex} = 390 and 410 nm, the solvation relaxation time is the same, that is, τ_L = 2200 for both the cases but is significantly different (τ_L= 1100) when excitation wavelength used is 420 nm. The need for two distinct solvent relaxation times, viz. τ_L= 2200 (ps) and τ_L = 1100 ps, to reproduce the experimental results of $S(t)$ (Figure 5) indicates the presence of two distinct environment around the solute particle (coumarin 480). Again, another very

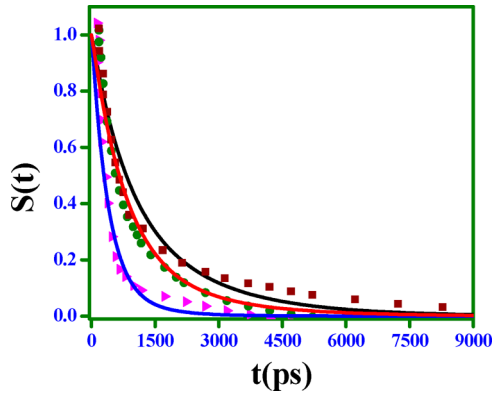

Figure 5. Plot of $S(t)$ versus time t in picoseconds (ps) for the parameters: k_m = 4.0 eV, λ_T = 0.4 eV, T = 300 K, and κ = 0.05. The parameters τ_L = 2200 ps corresponding to the excitation wavelengths λ_{ex} = 390 and 410 nm and τ_L = 1100 ps for λ_{ex} = 420 nm. The results based on the new relation (eq 9) are shown by the solid lines. The black, red, and blue solid lines correspond to the excitation wavelength λ_{ex} = 390, 410, and 420 nm. The experimental[22] results are plotted as square (□), circle (○), and triangle (△) corresponding to the excitation wavelengths λ_{ex} = 390, 410, and 420 nm.

interesting observation from Figure 5 is that the solvation dynamics dramatically slows down by almost three orders of magnitude (Figure 5) in comparison with the same in bulk water (~1 ps) due to highly restricted motion of the solvent molecules in the water pool and inside the vesicle but near the interface in comparison with free water in bulk.

To summarize, this is the first time a simple 1D unified theory (eqs 1, 2, 5, 6, and 9) has been developed to study the effect of innumerable Franck−Condon states through the single parameter excitation wavelength λ_{ex} on NESD and ETRK, which was missing in the existing theories.[1−16] It is also able not only to explain the origin of break down of Marcus theory[11−16] for ETRK and linear response theory for solvation dynamics[1−10] but also to predict the effect of λ_{ex} on ETRK and NESD observed in experiment,[17−24] whereas existing theories[1−16] are unable to predict the same. Most importantly, the calculated results for $S(t)$ (eq 9) are also found to be in excellent agreement with the large set of experimental results[22−24] for different λ_{ex} and significantly outperform the results of the same obtained based on linear response theory to describe solvation dynamics.[1−10] The present unified theory thus not only advances the knowledge of scientific community for photo-induced nonequilibrium processes but also provides a scheme to the experimentalist for precise control of the same.

AUTHOR INFORMATION

Corresponding Author

*E-mail: alokk@barc.gov.in.

ORCID

Alok Kumar Samanta: 0000-0002-8348-3866

Swapan K. Ghosh: 0000-0002-9152-4920

Notes

The authors declare no competing financial interest.

ACKNOWLEDGMENTS

Dr(s). Arup K. Pathak, K. R. S. Chandrakumar, and B. Modak are gratefully acknowledged for their constant encouragement. The work was supported by DAE under project XII-N-R&D-

DOI: 10.1021/acs.jpclett.7b01938
J. Phys. Chem. Lett. 2017, 8, 4545−4549

02.04/Theoretical & Computational Chemistry of Complex Systems.

REFERENCES

(1) Jimenez, R.; Fleming, G. R.; Kumar, P. V.; Maroncelli, M. Femto second dynamics of water. *Nature* **1994**, *369*, 471−473.
(2) Egorov, S. Ion Solvation dynamics in supercritical fluids. *Phys. Rev. Lett.* **2004**, *93*, 023004.
(3) Bragg, A. E.; Cavanagh, M. C.; Schwartz, B. J. Linear response breakdown in solvation dynamics induced by atomic electron-transfer reactions. *Science* **2008**, *321*, 1817−1822.
(4) Nandi, A.; Bhattacharyya, K.; Bagchi, B. Dielectric relaxation and solvation dynamics of water in complex chemical and biological systems. *Chem. Rev.* **2000**, *100*, 2013−2046.
(5) Bagchi, B.; Chandra, A. Polarization relaxation, dielectric dispersion and solvation dynamics in dense dipolar liquid. *J. Chem. Phys.* **1989**, *90*, 7338−7345.
(6) Roy, S.; Bagchi, B. Microscopic theory of ion solvation dynamics in liquid methanol. *J. Chem. Phys.* **1994**, *101*, 4150−4155.
(7) Wolynes, P. Linearized microscopic theories of nonequilibrium solvation. *J. Chem. Phys.* **1987**, *86*, 5133−5136.
(8) Maroncelli, M.; MacInnis, J.; Fleming, G. R. Polar Solvent dynamics electron-transfer reactions. *Science* **1989**, *243*, 1674−1681.
(9) Carter, E. A.; Hynes, J. T. Solvation dynamics for an ion pair in a polar solvent: Timedependent fluorescence and photochemical charge transfer. *J. Chem. Phys.* **1991**, *94*, 5961−5979.
(10) Onsager, L. Reciprocal relations in irreversible processes. *Phys. Rev.* **1931**, *37*, 405−426.
(11) Tachiya, M.; Murata, S. Non-Marcus energy gap dependence of back electron transfer in contact ion pairs. *J. Am. Chem. Soc.* **1994**, *116*, 2434−2436.
(12) Bauer, A.; Westkamper, F. S.; Grimme, S.; Bach, T. Catalytic enantioselective reactions driven byphotoinduced electron transfer. *Nature* **2005**, *436*, 1139−1140.
(13) Markel, F.; Ferris, N.; Gould, I. R.; Myers, A. B. Mode-specific vibrational reorganization Energies accompanying photoinduced electron transfer in the hexamethylbenzene/tetracyanoethylene charge-transfer complex. *J. Am. Chem. Soc.* **1992**, *114*, 6208−6219.
(14) Bagchi, B.; Gayathri, N. Interplay between ultrafast polar solvation and vibrational dynamics in electron transfer reactions:Role of high-frequency vibrational modes. *Adv. Chem. Phys.* **1999**, *107*, 1−80.
(15) Gould, I. R.; Farid, S. Dynamics of bimolecular photoinduced electron-transfer reactions. *Acc. Chem. Res.* **1996**, *29*, 522−528.
(16) Marcus, R. A. Electrostatic free energy and other properties of states having nonequilibrium polarization I*. *J. Chem. Phys.* **1956**, *24*, 979−989.
(17) Fedunov, R. G.; Feskov, S. V.; Ivanov, A. I.; Nicolet, O.; Pages, S.; Vauthey, E. Effect of the excitation pulse carrier frequency on the ultrafast charge recombination dynamics of donor-acceptor complexes: Stochastic simulations and experiments. *J. Chem. Phys.* **2004**, *121*, 3643−3656.
(18) Nicolet, O.; Banerji, N.; Pages, S.; Vauthey, E. Vauthey, Effect of the excitation wavelength on the ultrafast charge recombination dynamics of donor-acceptor complexes in polar solvents. *J. Phys. Chem. A* **2005**, *109*, 8236−8245.
(19) Vauthey, E. Investigations of bimolecular photoinduced electron transfer reactionsin polar solvents using ultrafast spectroscopy. *J. Photochem. Photobiol., A* **2006**, *179*, 1−12.
(20) Mikhailova, V. A.; Ivanov, A. I.; Vauthey, E. Nonequilibrium charge recombination from the excited adiabatic state of donor-acceptor complexes. *J. Chem. Phys.* **2004**, *121*, 6463−6469.
(21) Ivanov, A. I.; Belikeev, F. N.; Fedunov, R. G.; Vauthey, E. The effect of excitation pulse carrier frequency on ultrafast charge recombination dynamics of excited donor−acceptor complexes. *Chem. Phys. Lett.* **2003**, *372*, 73−81.
(22) Sen, P.; Satoh, K.; Bhattacharyya, K.; Tominaga, K. Excitation wavelength dependence of solvation dynamics of coumarin 480 in a lipid vesicle. *Chem. Phys. Lett.* **2005**, *411*, 339−344.
(23) Sen, P.; Ghosh, S.; Mondal, S. K.; Sahu, K.; Roy, D.; Bhattacharyya, K.; Tominaga, K. A Femtosecond study of excitation-wavelength dependence of solvation dynamics in a vesicle. *Chem. - Asian J.* **2006**, *1*, 188−194.
(24) Mondal, S. K.; Sahu, S. K.; Bhattacharyya, K. Study of biological assembly by ultrafast fluorescence spectroscopy. *Rev. Fluoresc.* **2009**, *2007*, 157−177.
(25) Zwanzig, R. Memory Effects in irreversible thermodynamics. *Phys. Rev.* **1961**, *124*, 983−992.
(26) Garcia-Colin, L. S.; del Rio, J. L. A unified method for deriving kinetic equations in the statistical mechanics of irreversible processes I. Exact results. *J. Stat. Phys.* **1977**, *16*, 235−258.
(27) Patra, A.; Samanta, A. K.; Ghosh, S. K. Mapping the reaction dynamics in Liouville space onto a reaction coordinate space: A first-principle based theory. *Phys. Rev. E* **2011**, *83*, 026104.
(28) Patra, A.; Acharya, K. A.; Samanta, A. K. Projection of the Dynamics of Electron Transfer Reaction in Dual Space onto the One-Dimensional Slower Reaction Coordinate Axis. *J. Phys. Chem. B* **2015**, *119*, 11063−11067.
(29) Dhole, K.; Modak, B.; Samanta, A. K.; Ghosh, S. K. Theory of reversible electron transfer reactions in a condensed phase. *Phys. Rev. E* **2010**, *82*, 016110−11.
(30) Dhole, K.; Jena, N.; Samanta, A. K.; Ghosh, S. K. Electron transfer reactions in condensed phase: Effect of reversibility. *Phys. Rev. E* **2012**, *85*, 026105−11.

DOI: 10.1021/acs.jpclett.7b01938
J. Phys. Chem. Lett. 2017, 8, 4545−4549